

Supplementary Information

for

**First coordination compounds based on a *bis(imino nitroxide)* biradical and
4f metal ions: synthesis, crystal structures and magnetic properties**

Samira G. Reis^a, Matteo Briganti^b, Daniel O. T. A. Martins^a, Handan Akpinar^c, Sergiu Calancea^a, Guilherme P. Guedes^d, Stéphane Soriano^e, Marius Andruh^f, Rafael A. A. Cassaro^g, Paul M. Lahti^{c*}, Federico Totti^b and Maria G. F. Vaz^{a*}

^aInstituto de Química, Universidade Federal Fluminense, Niterói, 24020-150, RJ, Brazil.

^bDipartimento di Chimica, Università degli studi di Firenze, 50019, Sesto Fiorentino, Firenze, Italy

^cDepartment of Chemistry, University of Massachusetts, Amherst, Massachusetts, 01003 USA

^dInstituto de Ciências Exatas, Departamento de Química, Universidade Federal Rural do Rio de Janeiro, Seropédica, 23851-970, RJ, Brazil.

^eInstituto de Física, Universidade Federal Fluminense, Niterói, 24210-346, RJ, Brazil

^fInorganic Chemistry Laboratory, Faculty of Chemistry, University of Bucharest, Str. Dumbrava Rosie nr. 23, 020464-Bucharest, Romania.

^gInstituto de Química, Universidade Federal do Rio de Janeiro, Rio de Janeiro, 21941-909, RJ, Brazil.

Table of Contents

Table S1: Hydrogen-bonding geometry for 1-3	S2
Table S2: Summary of data collection and refinement for 4	S3
Figure S1: Experimental powder X-ray diffraction for 1 (black) and 2 (blue), with pattern simulated from crystal structure of 1 (red)	S4
Figure S2: Experimental powder X-ray diffraction for 4 (black) and 5 (blue), with pattern simulated from crystal structure of 5 (red)	S5
Figure S3: M vs H/T plot at different temperatures for 2	S6
Figure S4: M vs H/T plot at different temperatures for 3	S7
Figure S5: M vs H plot for 5 at 4.0 K	S7
Figure S6. Thermal dependence of in-phase and out-of-phase susceptibility for 2 ($H_{ext}=0$)	S8
Figure S7. Arrhenius plot from the out-of-phase peak maxima at 2 kOe external field for 2	S9
Figure S8. Isothermal ac magnetic susceptibilities at varying ac frequency at 2 kOe for 2	S10
Table S3: Contractions of the basis sets employed in the calculations.	S11
Table S4: Computed energy levels of Tb ion at CASSCF/RASSI-SO level.....	S11
Table S5: Tensor elements of the main anisotropy axis for Tb ^{III} and its orientation in the crystal frame.....	S12

Table S1. Hydrogen bonding parameters for **1-3**.

Compounds	$D\text{---H}\cdots A$	$D\text{---H}$	$H\cdots A$	$D\cdots A$	$D\text{---H}\cdots A$
1 (Ln = Gd)	O16—H16a…O7	0.85	2.43	2.928(7)	118
	O16—H16a…F17b	0.85	2.39	3.155(14)	150
	O8—H8a…F26	0.85	2.36	3.124(7)	150
2 (Ln = Dy)	O16—H16a…O7	0.87	2.45	2.934(15)	115
	O16—H16a…F18	0.87	2.54	3.279(18)	144
	O16—H16b…O1	0.87	1.89	2.665(14)	148
	O8—H8a…F25	0.87	2.36	3.155(14)	151
	O8—H8b…O9	0.87	2.12	2.634(15)	117
	O8—H8b…O15	0.87	2.49	3.082(17)	155
	O8—H8b…O16	0.87	2.44	3.247(15)	126
3 (Ln = Tb)	O8—H8b…N4	0.85	1.95	2.756 (7)	157
	O8—H8a…O7	0.85	2.39	2.756 (7)	107

Table S2: Summary of data collection and refinement for **4**

Chemical formula	C ₃₅ H ₃₂ F ₁₈ GdIN ₄ O ₉
Formula Mass	1278.78
Crystal system	Monoclinic
<i>a</i> /Å	15.273 (5)
<i>b</i> /Å	12.299 (5)
<i>c</i> /Å	25.354 (5)
α^o	90
β^o	100.252 (5)
γ^o	90
Unit cell volume/Å ³	4687 (3)
Temperature/K	150
Space group	<i>P</i> 2 ₁ /c
<i>Z</i>	4
Radiation type	MoKα
μ/mm^{-1}	2.198
Reflections measured	56324
Independent reflections	9619
R_{int}	0.064
R_I values ($I > 2\sigma(I)$)	0.183
$wR(F^2)$ values ($I > 2\sigma(I)$)	0.331
R_I values (all data)	0.211
$wR(F^2)$ values (all data)	0.346
Goodness of fit on F^2	1.137

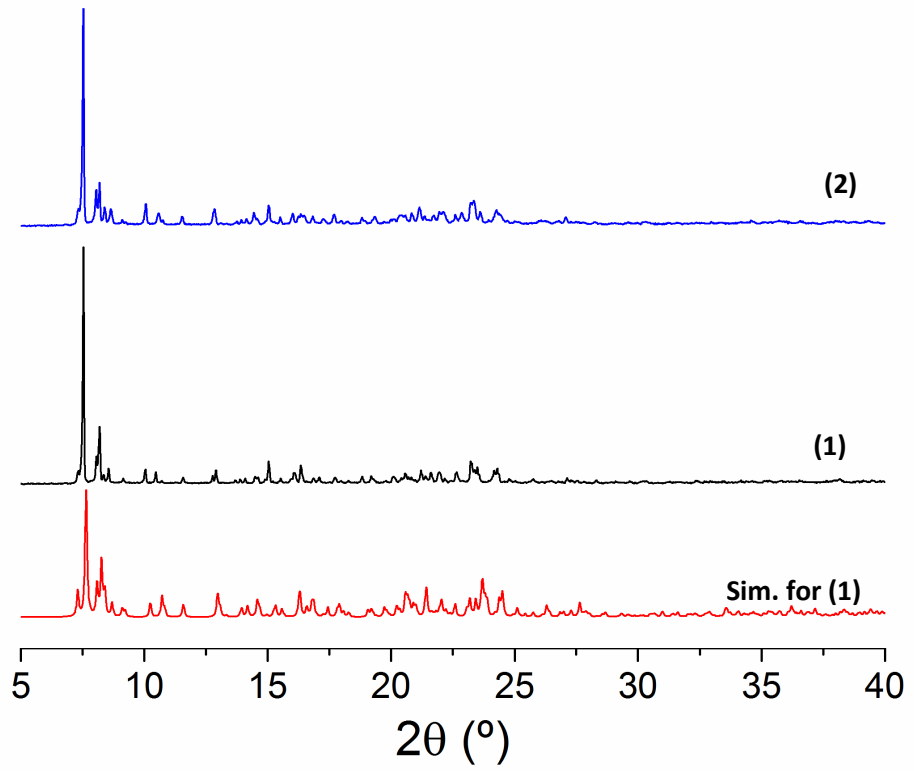


Figure S1. Experimental powder X-ray diffraction for **1** (black) and **2** (blue) with pattern simulated from crystal structure of **1** (red).

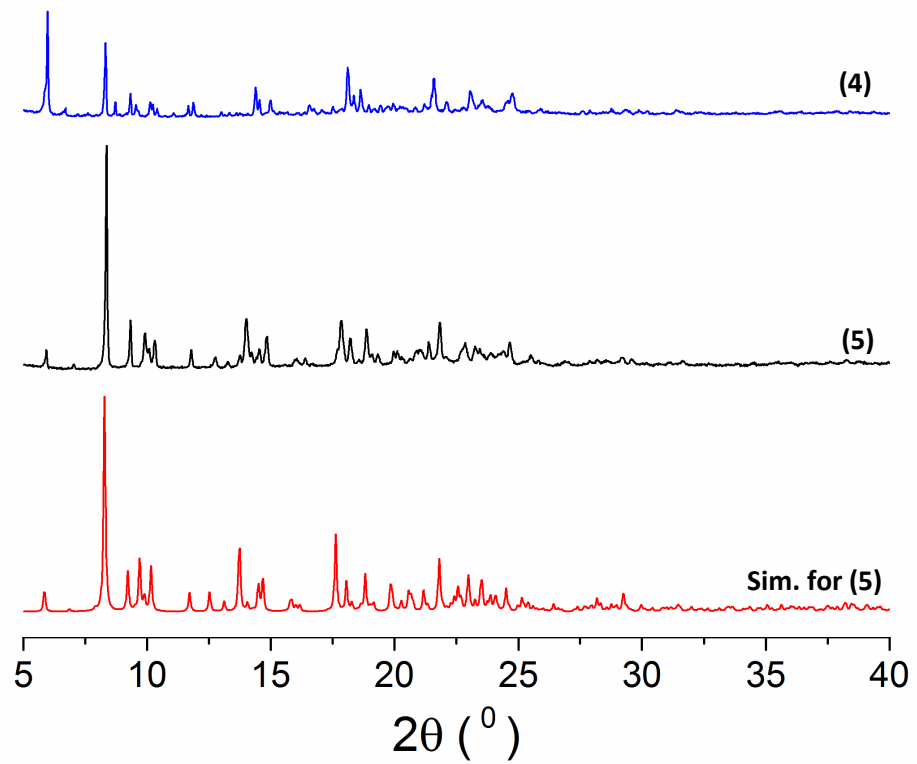


Figure S2. Experimental powder X-ray diffraction for **4** (blue) and **5** (black) with pattern simulated from crystal structure of **5** (red).

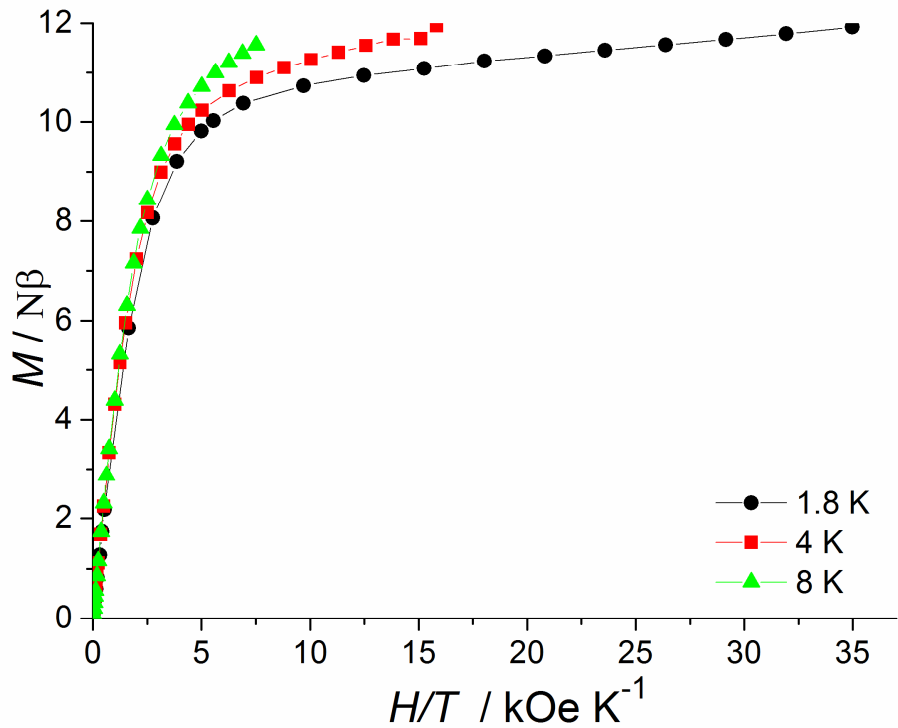


Figure S3. M vs H/T plot at different temperatures for **2**.

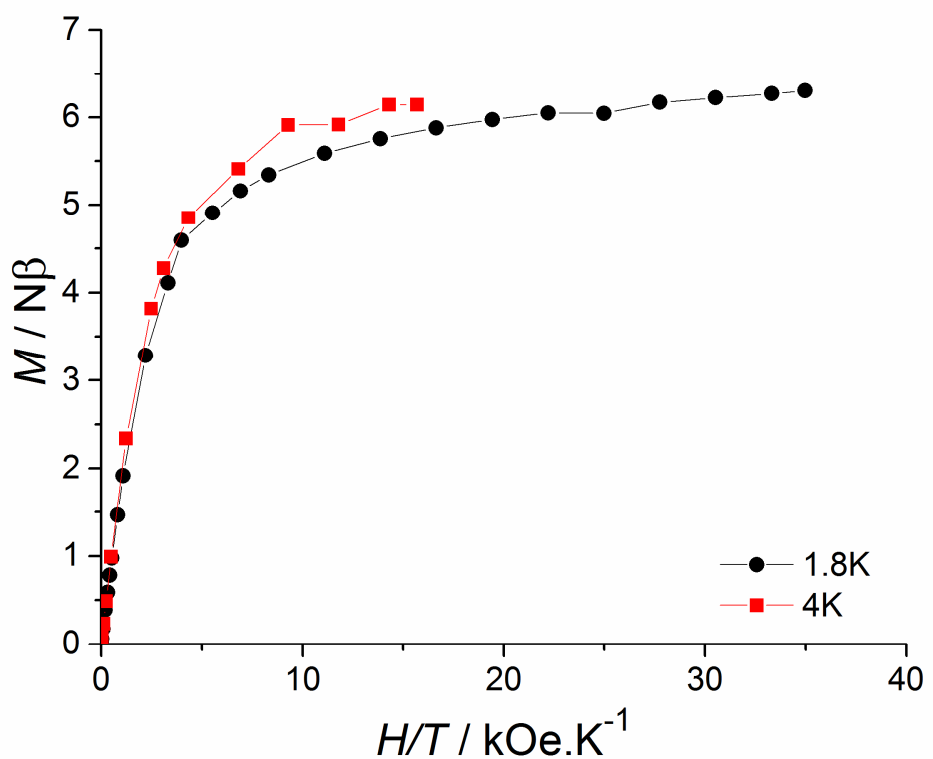


Figure S4. M vs H/T plot at different temperatures for **3**.

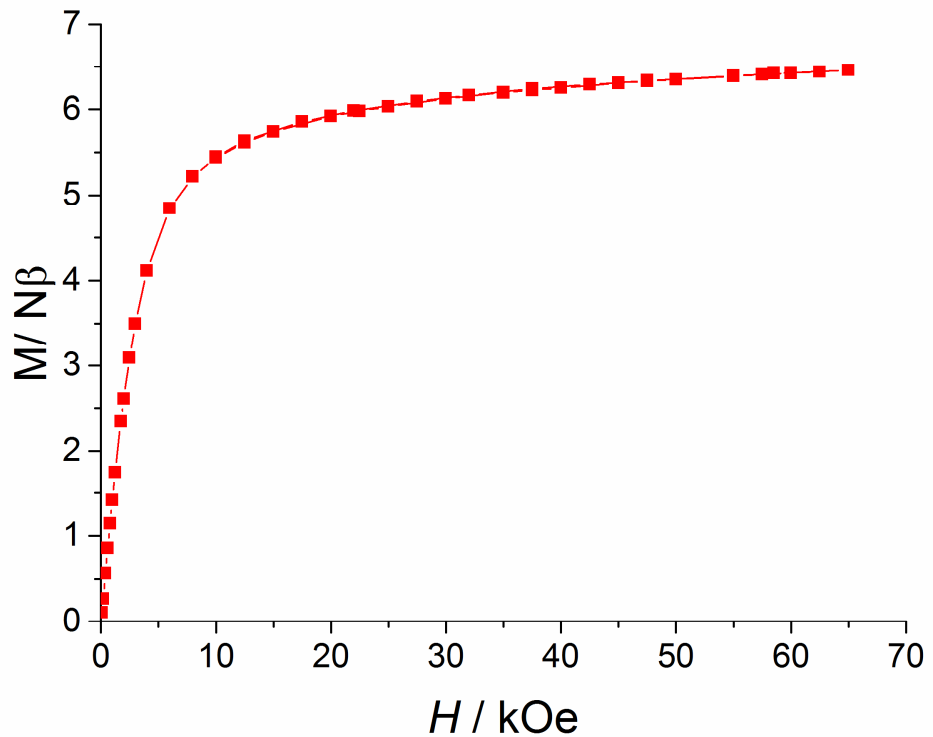


Figure S5. M vs H plot for **5** at 4.0 K.

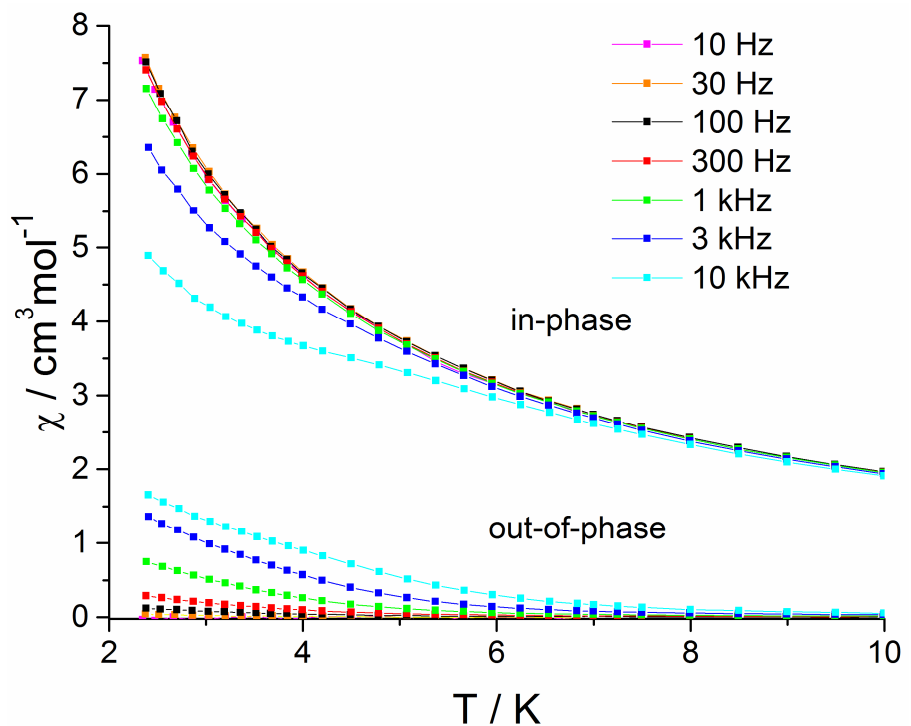


Figure S6. Thermal dependence of the in-phase and out-of-phase susceptibility components for **2** at zero external field.

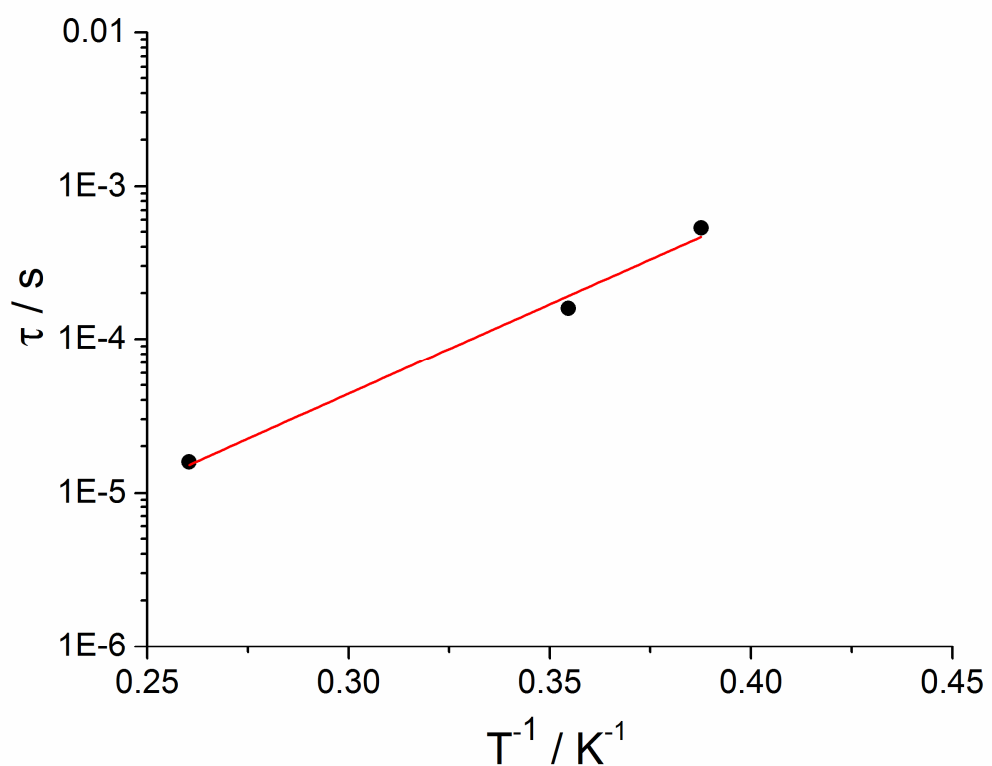


Figure S7. Arrhenius plot from the out-of-phase peak maxima at 2 kOe external field for **2**.

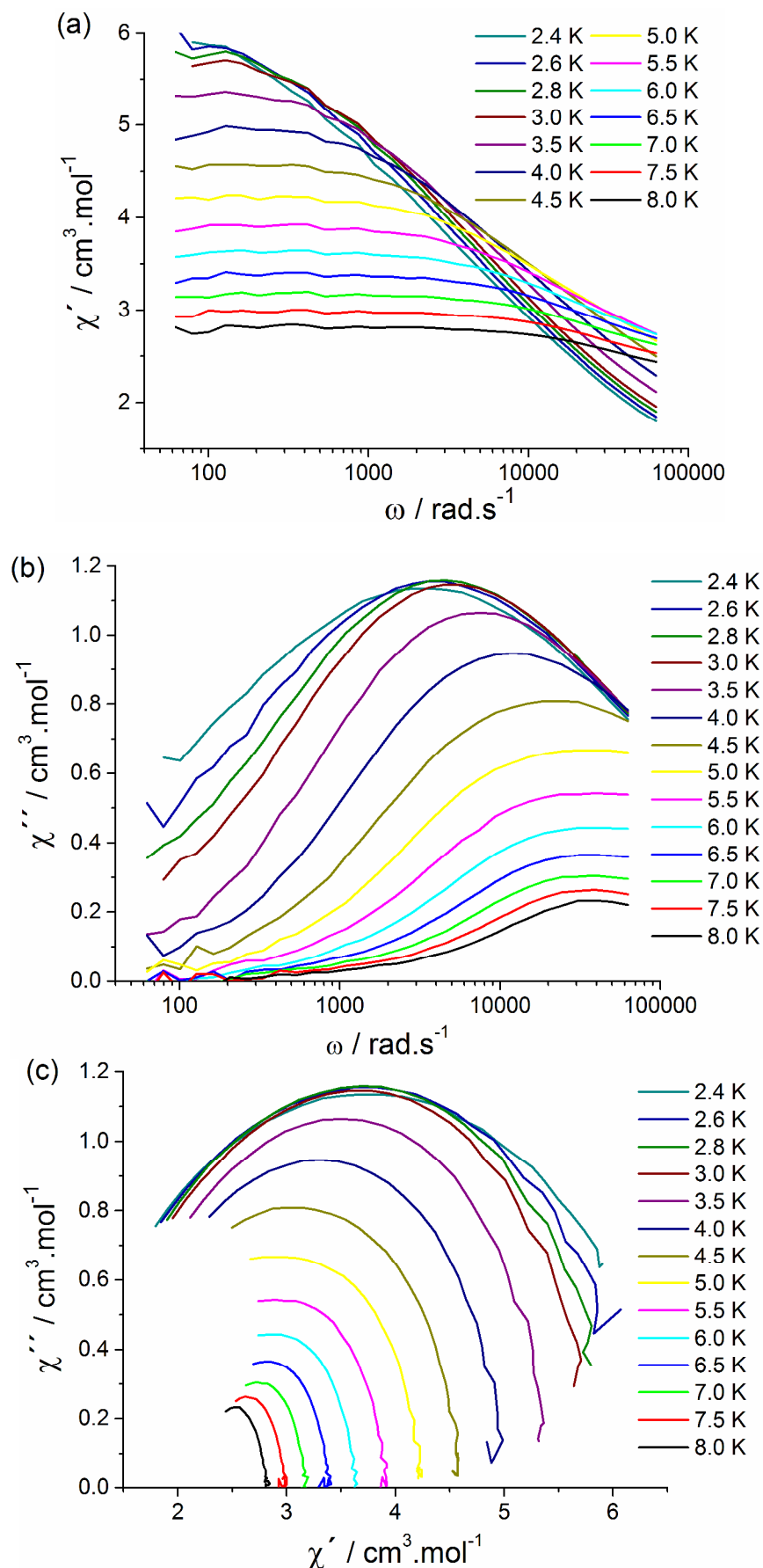


Figure S8. Isothermal ac magnetic susceptibilities at varying ac frequency at 2 kOe for **2**: (a) χ' vs omega, (b) χ'' vs omega, (c) Cole-Cole plot (χ'' vs χ').

Table S3: Contractions of the basis sets employed in the calculations.

Atom	Contraction
Tb	TB.ANO-RCC...8S7P5D3F2G1H
O	O.ANO-RCC...4S3P2D1F
N	N.ANO-RCC...4S3P2D1F
C	C.ANO-RCC...3S2P1D
I	I.ANO-RCC...6S5P2D
F	F.ANO-RCC...3S2P
H	H.ANO-RCC...2S

Table S4: Computed energy levels of Tb^{III} ion at CASSCF/RASSI-SO level.

Energy levels (cm ⁻¹)	
1	0.000
2	0.347
3	89.845
4	90.703
5	109.513
6	111.803
7	191.479
8	201.404
9	268.620
10	280.485
11	315.920
12	410.602
13	414.523
14	1805.832
15	1808.998
16	1952.147
17	1959.141
18	1987.640
19	1992.251
20	2018.422
21	2043.449
22	2053.471
23	2118.413
24	2126.052
25	3328.146
26	3360.915
27	3388.707
28	3420.729
29	3451.700
30	3521.379
31	3565.893
32	3585.359
33	3626.162
34	4594.044
35	4606.628
36	4632.199
37	4682.828
38	4690.107
39	4711.278
40	4724.530
41	5415.617
42	5498.623
43	5566.550
44	5686.732
45	5689.230
46	6042.855
47	6219.226
48	6253.625
49	6477.807

Table S5: Tensor elements of the main anisotropy axis for Tb^{III} and its orientation in the crystal frame.

	Value	a	b'	c*
g_x	0.000000000	-.252700	.835891	-.487267
g_y	0.000000016	-.963926	-.261013	.052138
g_z	17.110777764	-.083601	.482865	.871695